PERGAMON

Deep-Sea Research II 46 (1999) 1597–1622

DEEP-SEA RESEARCH
PART II

Seasonal variations in the distribution of Fe and Al in the surface waters of the Arabian Sea

C.I. Measures*, S. Vink

Department of Oceanography, University of Hawaii, 1000 Pope Road, Honolulu, HI 96822, USA

Received 10 September 1997; received in revised form 29 September 1998; accepted 15 October 1998

Abstract

Concentrations of dissolved Al and Fe in the surface mixed layer were measured during five cruises of the 1995 US JGOFS Arabian Sea Process Study, Concentrations of both Al and Fe were relatively uniform between January and April, the NE Monsoon and the Spring Intermonsoon period, ranging from 2 to 11 nM Al (mean 5.3 nM) and 0.5 to 2.4 nM Fe (mean 1.0 nM). In July/August, after the onset of the SW Monsoon, surface water Al and Fe concentrations increased significantly (Al range 4.5–20.1 nM; mean = 10 nM, Fe range 0.57–2.4 nM; mean = 1.3 nM), particularly in the NE part of the Arabian Sea, as the result of the input and partial dissolution of eolian dust. Using the enrichment of Al in the surface waters, we estimate this is the equivalent to the deposition of 2.2–7.4 g m^{-2} dust, which is comparable to values previously estimated for this region. Approximately one month later (August/September), surface water concentrations of both Al and Fe were found to have decreased significantly (mean Al 7.4 nM, mean Fe 0.90 nM) particularly in the same NE region, as the result of export of particulate material from the euphotic zone. Fe supply to the surface waters is also affected by upwelling of sub-surface waters in the coastal region of the Arabian Sea during the SW Monsoon. Despite the proximity of high concentrations of Fe in the shallow sub-oxic layer, freshly upwelled water is not drawn from this layer and the NO_3/Fe ratio in the initially upwelled water is below the value at which Fe limitation is through to occur. Continued deposition of eolian Fe into the upwelled water as it advects offshore provides the Fe required to raise this ratio above the Fe limitation value.

1. Introduction

It is becoming increasingly important to understand the role that eolian deposition plays in supplying trace elements to the surface waters of the ocean, and the role that

* Corresponding author. Fax: 001-808-956-9225.
E-mail address: chrism@soest.hawaii.edu (C.I. Measures)

0967-0645/99/$ - see front matter
PII: S0967-0645(99)00037-5

this episodic supply plays in moderating biological processes. While it has been recognised for some time that the dust deposition process is the major geochemical pathway for supply of some elements, e.g., Al, Mn, Fe, to the remote surface ocean (Kremling, 1985; Statham and Burton, 1986; Measures et al., 1986; Duce and Tindale, 1991), the recent proposition that low Fe levels in some remote regions may limit surface water production (Martin and Fitzwater, 1988; Martin et al., 1990) adds new impetus for understanding the mechanisms by which such delivery is accomplished and the factors that control it. Further, the use of experimental additions of Fe to low-Fe regions to precipitate changes in biological interactions requires an a priori knowledge of the natural response of the surface ocean chemistry to episodic dust additions (Martin et al., 1994; Coale et al., 1996).

The potential connection between pulsed iron deposition to the surface of the ocean and carbon export from it, is particularly interesting because it may provide a non-linear feedback between surface ocean chemistry, biological processes and, through atmospheric CO_2 levels, climate. This connection may be non-linear because pulsed iron depositions may result in alteration in food web dynamics. A steady-state food web, in which small phytoplankton are kept in check by small zooplankton, results in low export production since most of the nutrients consumed in the photic zone are recycled through grazing (Banse, 1994). If rapid chemical changes occur in the surface of the ocean such that the growth of much larger phytoplankton is suddenly favoured, then the lack of appropriate grazers for the larger cells will lead to a population explosion. Lack of grazing also leads to a diminishment (or cessation) of recycling of the nutrient pool which in turn leads to the phytoplankton population crashing. The senescent population will settle out of the photic zone, taking its incorporated nutrients with it. The presumed connection of Fe to this disturbance process arises from the absolute Fe-requirement of phytoplankton for a variety of biochemical processes. The individual cell's Fe-requirement scales with the volume of the cell, but the ability to transport Fe from the surrounding water across the cell membrane scales with the surface area of the cell. Thus, at low ambient Fe concentrations small cells with high surface area-to-volume ratios are favoured (Sunda and Huntsman, 1997). The rapid addition of significant quantities of Fe to surface waters increases the ambient Fe concentrations and increases the ability of large cells with their less favourable surface-to-volume ratios to compete for the available Fe. In the absence of significant numbers of appropriate-sized grazers for this group, the large cells will find an advantage and their population will grow unchecked, leading to the crash and export process outlined above.

In terms of carbon and nutrient export, an important factor is the disturbance of quasi steady-state conditions by rapid changes in surface water chemistry. Thus, it is important to observe the response of the biogeochemical cycle to natural episodic additions of Fe to the photic zone. The deposition and partial dissolution of dust in the surface waters of the ocean is one such episodic mechanism, as is the upwelling of Fe-rich sub-surface waters. Direct determination of dust deposition at sea is extremely problematic, although measurements of suspended dust load can be coupled with scavenging ratios to estimate this parameter. Dissolved Al released into surface waters

through dust dissolution has been used successfully as a proxy to estimate dust deposition in the Atlantic Ocean (Measures and Brown, 1996).

The surface water of the Arabian Sea (AS) is an important region in which to study the complex interactions of biological processes with natural episodic injections of Fe into the photic zone. The AS experiences monsoonal eolian deposition, coastal and open ocean upwelling, as well as seasonal surges in primary production. In addition, because of the differential solubility of oxidised and reduced forms of Fe, the sub-surface, sub-oxic water of the region may play a significant role in moderating the normal chemical separation of Fe from N and P during the remineralisation of organic matter. The degree to which each of these processes interact in this ocean region will be of use in elucidating chemical and biological interactions in other, more iron impoverished, oceanic regimes.

The distribution of dissolved Al and Fe in the surface waters of the AS during the JGOFS cruises is the result of the interplay of various atmospheric, chemical, physical and biological processes many of which are still being examined. In this manuscript we will present a simple, first-order descriptive explanation of observed Al and Fe concentration changes coupled with a few simple calculations to demonstrate the feasibility of the various processes in controlling them. We expect that a more rigorous delineation of the processes will be possible when the other data sets from the AS are ready and available for interdisciplinary interpretation.

2. Methods

2.1. Analytical methods

Samples were collected for determination of dissolved Fe and Al on cruises TN043, 45, 49, 50 and 53 at most stations along the standard cruise track (Fig. 1). Throughout this paper references to the northern section will denote stations N1–N11 and the southern section will include stations S1–S15. During the 5 cruises, samples for vertical profiles were collected using trace metal clean techniques from two different sampling systems. During TN043 and TN045, and at stations N1–N7 during TN049, samples were obtained from 30-l Go-Flo bottles mounted on a trace metal-clean rosette (Hunter et al., 1996). Subsequent to the loss of this equipment during TN049, samples were obtained from 30-l Go-Flo bottles mounted on a trace metal-clean rosette (Hunter et al., 1996). Subsequent to the loss of this equipment during TN049, samples were obtained with 10-l Niskin bottles equipped with epoxy-coated springs mounted on an epoxy-coated rosette frame. Prior to the loss of the Go-Flo system, comparative sampling (Fig. 2) had shown that at the iron levels extant in the AS, the Niskin system was capable of collecting water samples that were not systematically different in Fe content from those of the Go-Flo system. Additional surface samples were collected between stations on all cruises using a towed fish system which peristaltically pumped surface water ($\sim$ 1 m depth) on board through Teflon-lined polyethylene tubing (Vink et al., in review). Sub-samples were collected from the tubing outlet on board. All surface water samples were filtered through 0.2 μm

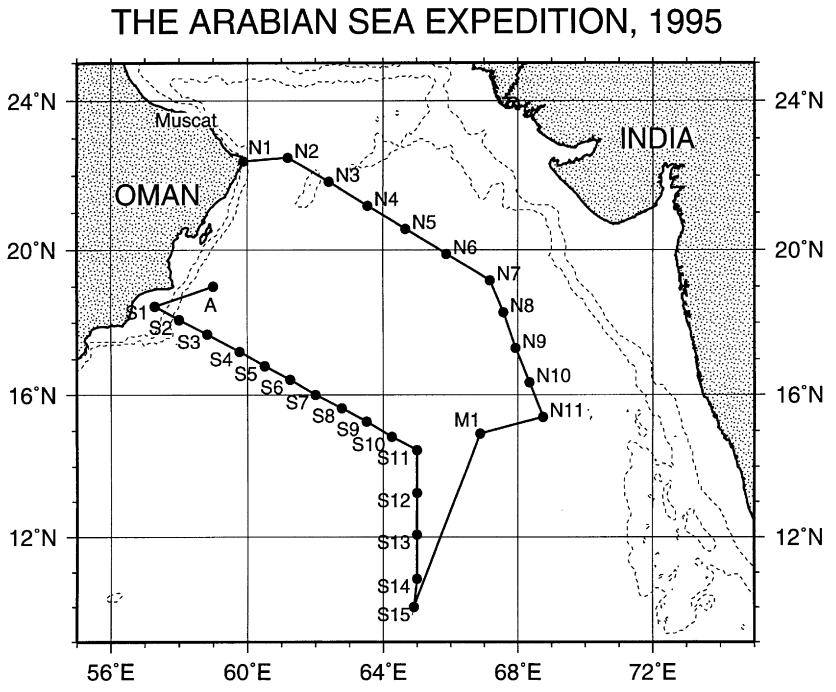

Fig. 1. Map of standard station locations occupied during the US JGOFS Arabian Sea Expedition. Bathymetric contours of 500 and 2000 m are also shown.

acid-leached filters (Gelman, Acro 50A), with the exception of profile samples collected between stations N1 and S4 during TN043 and all towed fish samples during TN043. Filtration of water samples was carried out in a class-100 laminar flow bench by peristaltically pumping each sample from its initial collection bottle through the filter into a sample bottle that was rinsed three times before sample collection. The same filter was used for several different samples, the first ~ 150 ml of filtrate from each new sample was discarded to eliminate cross-contamination by carry over.

Iron and A1 determinations were completed on board ship using the flow injection methods of Measures et al. (1995) and Resing and Measures (1994), respectively. Samples were acificied (1 ml 6N sub-boiled HCl l^{-1}) immediately prior to analysis and were preconcentrated for 1 min on an 8-hydroxyquinoline column. Dissolved Fe concentrations were determined by spectrophotometric detection of DPD-oxidized by Fe(III). The methodology has a typical precision of 2.5% at 0.35 nM and a detection limit of 0.025 nM. Dissolved Al concentrations were determined using spectrofluorometric detection of the fluorescent Al-lumogallion chelate. The method has a precision of 2% at 2.4 nM and a detection limit of ~ 0.15 nM. Each sample was analysed in duplicate, and the average concentration determined from these duplicates are reported. Results from samples where duplicate analyses differed by more

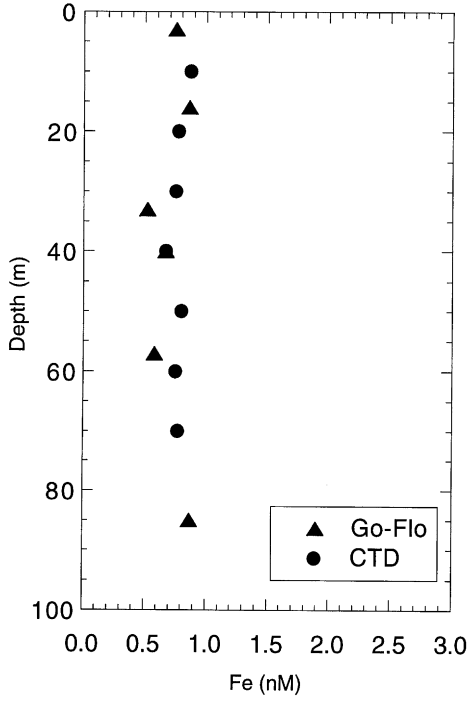

Fig. 2. Comparison of Fe concentrations determined from Go-Flo and Niskin sampling systems at station N7 occupied during TN045.

than 2–3% were discarded. Standard curves were run at least every 3–4 h, standards were made by addition of known amounts of a commercial Fe and Al standard (Fisher Chemical) to filtered acidified sub-surface seawater collected from one of the nearby stations. When necessary, the data for each day's run were drift-corrected to compensate for changes in instrument sensitivity.

2.2. Data analysis

Results from obviously contaminated samples, or samples in which poor precision of duplicates was observed, were eliminated from the data set ($\sim 10\%$ of data collected). At each station, the average concentration of each element in the mixed layer was calculated. The bottom of the mixed layer was defined by the depth at which there was a 0.125 kg m^{-3} change in sigma theta compared to the surface-water density; the values used are those presented in Morrison et al. (1998). Data from the surface towed fish are an average of duplicate determinations and this 1-m deep sample is assumed to be representative of the mixed layer concentration at that location. The average concentration determined at each station, combined with the individual surface water concentrations determined from the fish samples collected

between stations, were contoured using Generic Mapping Tools (Wessel and Smith, 1995). Contours were computed after fitting a minimum curvature surface with a maximum tension to the $0.5^\circ \times 0.5^\circ$ gridded data from each cruise (Smith and Wessel, 1990). Setting maximum tension in the surface grid constrains the solution so that local maximum or minimum values occur only at points where there are data (Smith and Wessel, 1990).

3. Results

The range and mean values of Al and Fe concentrations determined over the entire study area on each cruise are summarised in Table 1. Contour plots of the mixed layer average value of Al and Fe at each station and the values obtained using the surface towed fish are presented in Fig. 3 for each cruise.

On average over the study area both Al and Fe concentrations increased significantly between the Spring Intermonsoon cruise and the Mid-Southwest Monsoon cruise. This increase was followed by a dramatic decrease in the average concentrations of both elements determined approximately 1 month later during cruise TN050 (Table 1). Notable features of the distribution of each element on each cruise and changes in the distributions between the cruises as shown in the contour plots (Fig. 3) are outlined below.

3.1. Late Northeast Monsoon (TN043, January 8–Febuary 5, 1995)

During this cruise, convective cooling of the NE Monsoon resulted in deep mixed layers over much of the regions (37–113 m, average 81 m).

Surface Al concentrations were generally low (3–11 nM, Fig. 3a), cf. Atlantic Ocean where the range of surface water values is 20–80 nM. Highest values (7–11 nM) were found in the northern and eastern stations (N1–N11), and the extreme southern stations (S15–S13). The lowest values were found along the southern section and decreased from $\sim$ 5–7 nM (S11–S7) to $\sim$ 3 nM in the Omani coastal region (S1–S3). The overall pattern is a gradient across the AS of decreasing concentrations from NE to SW.

For Fe, the surface water distribution was less uniformly graded (Fig. 3b). Highest concentrations were found along the western part of the AS (generally $>$ 1nM) – most notably along the western end of the northern section (N1–N7, average $\sim 1.4 \pm 0.5$ nM, $n = 6$) and along the western end of the southern section (S5–S1, average 1.1 ± 0.3 nM, $n = 19$). Lower values were found in the eastern and southern part of the region (N9–S7, average 0.78 ± 0.2 nM, $n = 27$).

3.2. Spring Intermonsoon (TN045, March 7–April 4, 1995)

During TN045, mixed layer depths along the northern section N1–N6 were similar to those of TN043, while the depth of the mixed layer of the eastern and southern AS had shallowed. This shoaling of the mixed layer was most noticeable along the

Table 1
Range and average concentration of Al and Fe determined in the Arabian Sea during each cruise

Cruise	Season	Mixed layer depth range (m)	Al Conc. range (nM)	Avg Al Conc. (mean ± 1 s.d.) [n]	Fe Conc. range (nM)	Avg Fe Conc. (mean ± 1 s.d.) [n]
TN043 January 8–February 5	Late NE monsoon	10–118	2.77–11.28	5.32 ± 2.45 [176]	0.48–2.38	1.01 ± 0.41 [170]
TN045 March 7–April 4	Spring Inter-monsoon	10–152	2.1–9.6	5.26 ± 2.35 [44]	0.50–1.80	0.98 ± 0.34 [64]
TN049 July 17–August 15	Mid SW monsoon	10–148	4.5–20.1	9.98 ± 3.65 [131]	0.57–2.40	1.31 ± 0.51 [139]
TN050 August 18–September 15	Late SW monsoon	6–114	2.13–16.92	7.39 ± 2.23 [199]	0.48–1.67	0.91 ± 0.24 [206]
TN053 October 28–November 26	Early NE monsoon	14–73	2.28–13.73	5.34 ± 2.95 [257]	0.43–2.93	1.05 ± 0.40 [258]

Note: The mean concentration for each element was calculated as the average concentration determined at each station and values determined from the towed fish between stations. [n] is the number of values used to determine each average. Results from samples taken away from the standard JGOFS sample grid were not included in the average calculated for TN053. The range of mixed layer depths determined on each cruise by Morrison et al. (1998) is also tabulated.

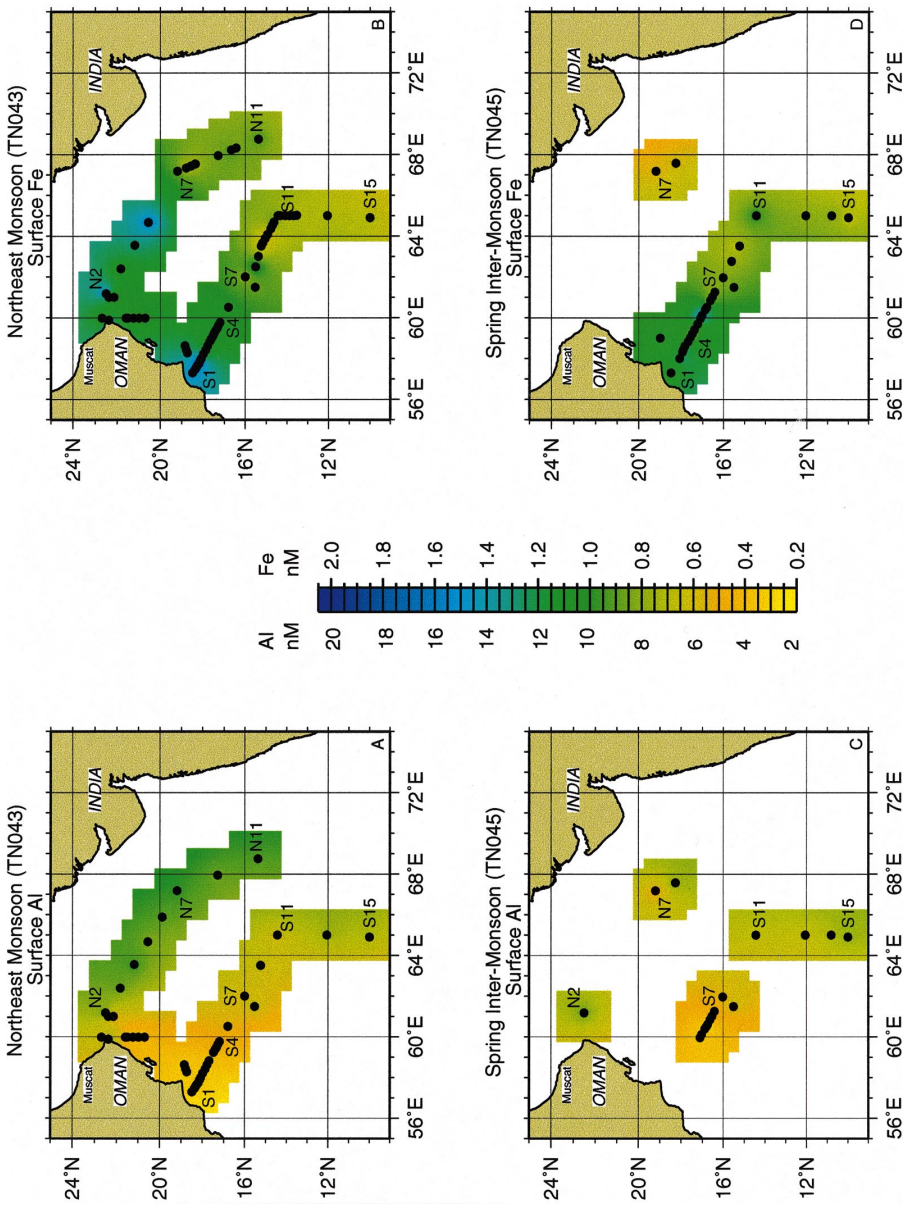

Fig. 3. Contoured mixed layer distributions of Al and Fe concentrations for each cruise. Sample locations are shown by (•) and the location of selected stations are noted by text.

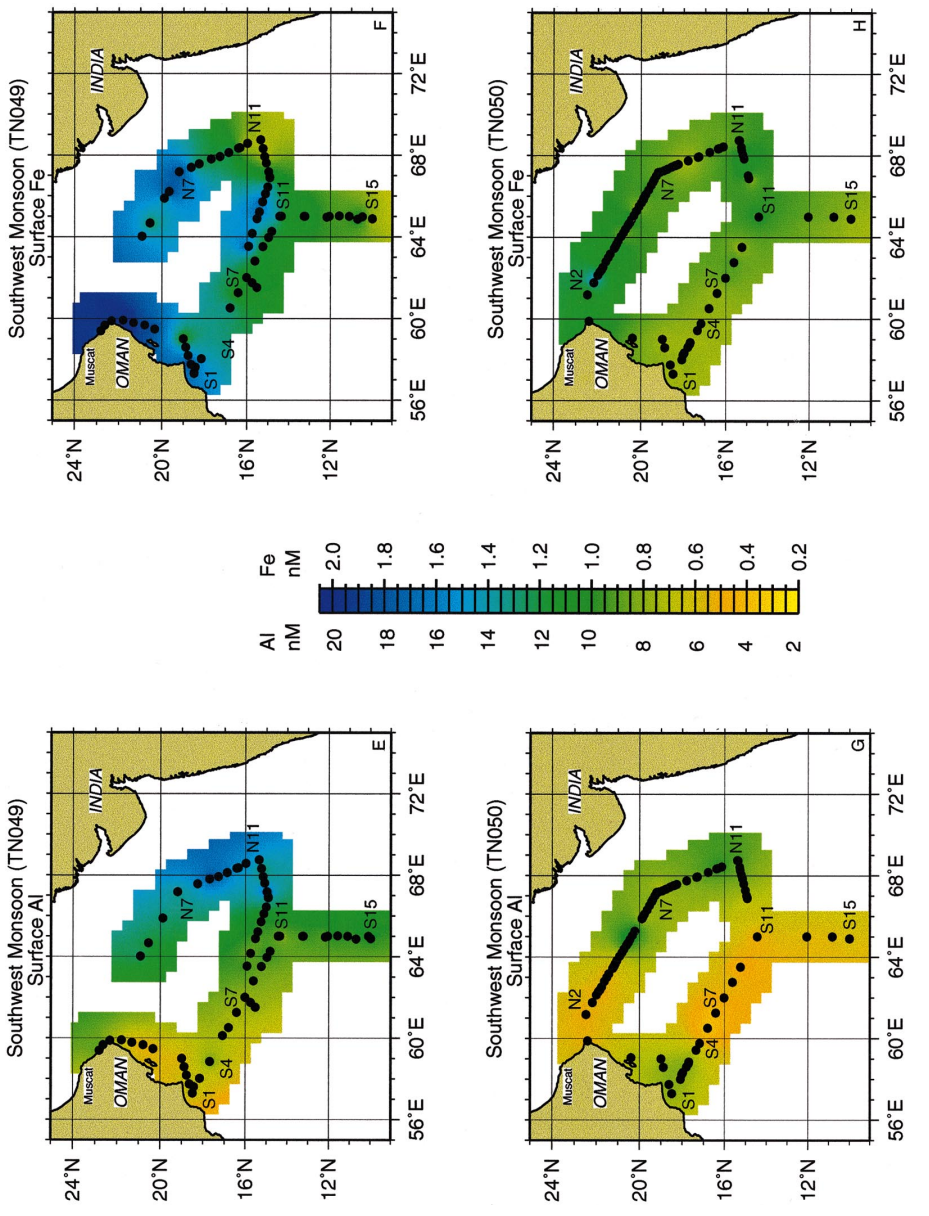

Fig. 3. Continued.

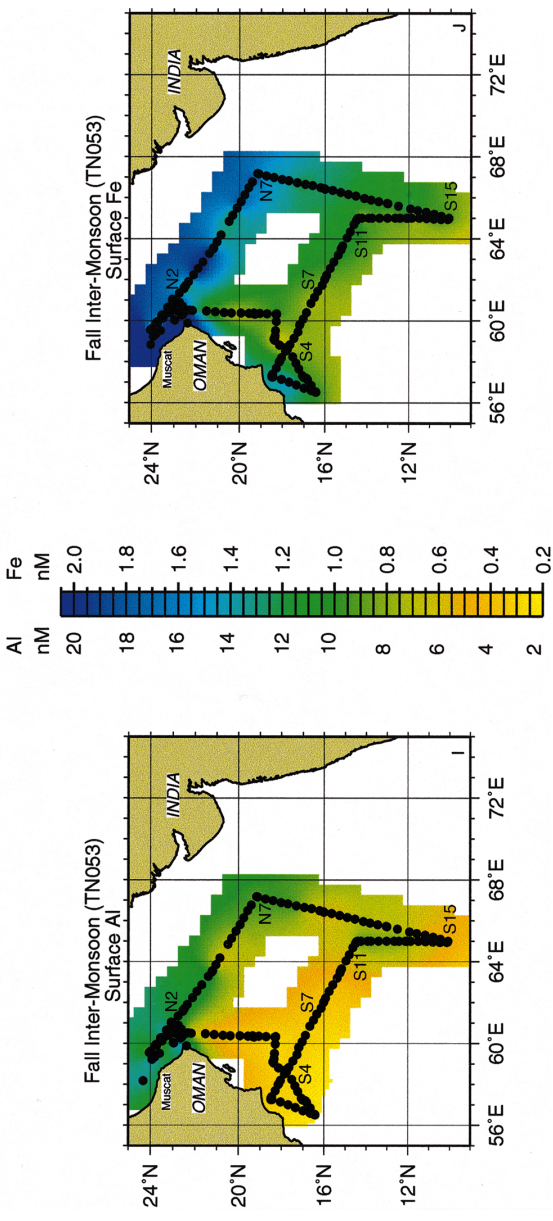

Fig. 3. Continued.

southern transect where mixed layer depths of < 30 m were observed between S11 and S1.

During this cruise equipment problems led to limited sampling along the northern transect and also at the western end of the southern section. Despite the limited data set, Al concentrations appeared to have changed very little between the two cruises and were in the 2–11 nM range (Fig. 3c). An exception to this was an isolated region of extremely low Al (3 nM) at N7. In regions where there is data coverage for both cruises, Al values changed generally by < 2 nM. The region of low Al appears to have spread slightly west from the coast along the southern section.

Iron values at the northern stations N7 and N8 were somewhat lower (~ 0.5 nM) than during TN043, while southern values (S15–S13) were very similar (0.6–0.9 nM). Low values (~ 0.6 nM) persisted along the southern section between stations S9–S6 (as during TN043), while higher values (~ 1.2 nM) were observed closer to the coast between S5 and S1. These latter values were slightly higher than those seen during TN043. In general, for most of the region Fe values were within 0.3 nM of those seen during TN043.

3.3. *Mid Southwest Monsoon (TN049, July 17–August 15, 1995)*

The onset of the SW Monsoon between TN045 and TN049 had a considerable effect on the structure of the near-surface water column. The mixed layers of the northern stations (N1–N6) shoaled to 10–50 m, and extremely deep mixed layers (80–110 m) were found between S15 and S3 with a small region of shallow mixed layers at S7–S6. Along the Omani coast section (S1–S2), shallow mixed layers and low surface water temperatures indicated the onset of upwelling.

Between TN045 and TN049, there were significant changes in both the magnitude and distribution of Al in surface water. The general pattern of east-west gradient seen during TN043, and less distinctly during TN045, was preserved. Aluminium concentrations increased across the entire AS, especially in the northeast (N7–N11), where values ranged from 13 to 20 nM (mean 15.5 nM) with significant mesoscale variability (Fig. 3e). There was also significant variation in surface Al along the southern section, with most values ranging from ~ 9 nM at S11 to ~ 7 nM along the Omani coast (S1). Within this section, there was also a region of somewhat lower Al values (average 6.8 nM) at stations S6 and S7 coincident with the region of shallow mixed layers. In the extreme southern area (S15–S13), Al values were ~ 10 nM. Examining stations that have Al data for both TN043 and TN049 shows that increases of 5–9 nM were seen in the NE stations N8–N11, and increases of 3–4 nM were seen in the southern area (S15–S11). Along the southern section (S9–S4), the increases were relatively small (1.5–2.0 nM), but larger increases (3–6 nM) occurred in the coastal region, (S1–S3).

Surface water Fe values also increased between TN045 and TN049. The overall distribution reveals significant small-scale horizontal variability superimposed upon a background gradient of high northern to lower southern values (Fig. 3f). Along the western end of the northern section (N5–N9), mixed layer values were mostly above 1 nM, with the region around N7 above 2.0 nM. Along the southern section (S11–S1), Fe values averaged 1.3 nM. A patch of low values (~ 0.9 nM) was seen at S6 and S7,

the region of shallow mixed layers described above. In the most southern area, Fe values dropped significantly from 1.44 nM at S12 to 0.6 nM at S15. Examining stations that have Fe data in both TN043 and TN049, it can be seen that the changes in Fe concentrations across the area were quite variable. Along the northern section, Fe concentrations generally increased by up to 1.23 nM, around N7, the region of high Fe during TN043. Along the central southern section (S2–S13) Fe increased by $\sim$ 0.3 nM.

3.4. Late Southwest Monsoon (TN050, August 18–September 15, 1995)

The continuation of the SW Monsoon during TN050 had very little effect on the mixed layer dynamics of the region. Northern section mixed layers deepened slightly, while continued upwelling led to shallower mixed layers along the Omani coast.

Surface Al concentrations underwent a dramatic decline between these two successive cruises. During TN050 in the east (N5–N11), surface water values generally ranged between 6–10 nM (mean 7.9 nM) (Fig. 3g). Vertical profiles of Al from cruises TN043, TN049 and TN050 at station N5 show the elevated Al concentrations in the upper 50 m of the water column during TN049. Below 50 m depth, Al concentrations were lower and similar values were observed on each cruise (Fig. 4). In the southern area and the central portion of the southern section (S15–S5), values were generally 4–6 nM (mean 4.5 nM). This distribution was similar to that seen in TN043 with the exception of a region of elevated Al values ($\sim$ 7–9 nM) along the Omani coast (S3–S1) during TN050. The overall changes in surface water values between TN049 and TN050 ranged from decreases of $\sim$ 5–9 nM Al in the eastern parts of the northern and southern sections to increases of $\sim$ 1 nM in the coastal region (S1–S2).

Surface water Fe concentrations also showed a dramatic decline during this period. Along the northern section (N1–N11), Fe concentrations averaged 1.0 ± 0.2 nM ($n = 55$), while along the southern section (S15–S1) they averaged 0.8 ± 0.2 nM ($n = 20$) (Fig. 3h). The magnitude of the Fe concentration change between TN049 and TN050 was quite variable, probably reflecting the heterogeneity in the TN049 distributions. Fig. 5 shows a plot of the gridded data of TN050 minus the gridded data of TN049. Between N6 and N9, decreases of 0.2 to 1.0 nM were seen. Small increases in Fe were seen at N10 and N11. At S15, Fe increased slightly while there was no change at S13. Decreases of $\sim$ 0.4 nM were seen at the eastern end of the southern section (S11–S9) with little or no change seen between S6 and S8. Decreases of $\sim$ 0.6 nM were seen between S5 and S1, and additional towed fish samples along the Omani coastal region indicated decreases of up to 1 nM.

3.5. Early Northeast Monsoon (TN053, October 28–November 26, 1995)

Cessation of the SW Monsoon led to a shoaling of the deep mixed layers of the eastern and southern AS. The cessation of upwelling along the Omani coast led to a deepening of the mixed layers in the region.

The bio-optics sampling strategy during TN053 resulted in only limited re-occupation of the standard JGOFS stations, but permitted a high density of the surface

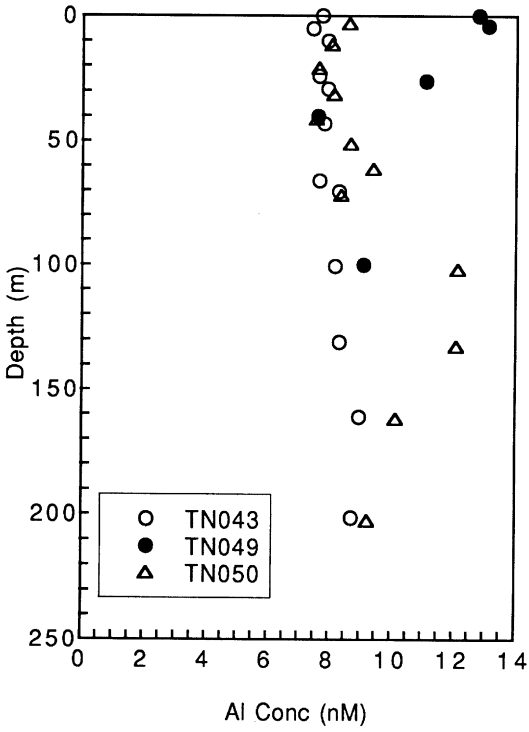

Fig. 4. Vertical profiles of dissolved Al concentrations determined at station N5 during 3 cruises, TN043 (late Northeast monsoon), TN049 (mid-Southwest monsoon) and TN050 (late Southwest monsoon).

sampling from the towed fish. During this cruise, surface water Al distributions showed a similar distribution to TN050 in the eastern part of the study area with typical values of 6–11 nM (Fig. 3g and Fig. 3i). The high Al region seen during TN050 along the Omani coast disappeared, with typical values of 2–3 nM from S7 to the Omani coast. The intense surface water sampling during this bio-optics cruise indicated fairly high values of Al along the eastern part of the northern section and into the Persian Gulf, where concentrations were typically in the range of 13–20 nM. Since few of the stations overlap between TN050 and TN053, it is difficult to assess station-by-station changes. However, the overall changes in the surface water between these two cruises ranged from increases of 4–6 nM Al in the northern section to reductions of 2–5 nM in the eastern part of the southern section near the Omani coast.

Fe values increased slightly between TN050 and TN053 mostly in the northern area (Fig. 3h and Fig. 3j). Fe concentrations were 0.8–1.2 nM along most of the southern section (S15–S1), with a patch of elevated values (1–1.5 nM) along the western end of the track at the Omani coast. High-density sampling along the northern transect and into the Persian Gulf shows high values ($>$ 3 nM) in the latter region and values of

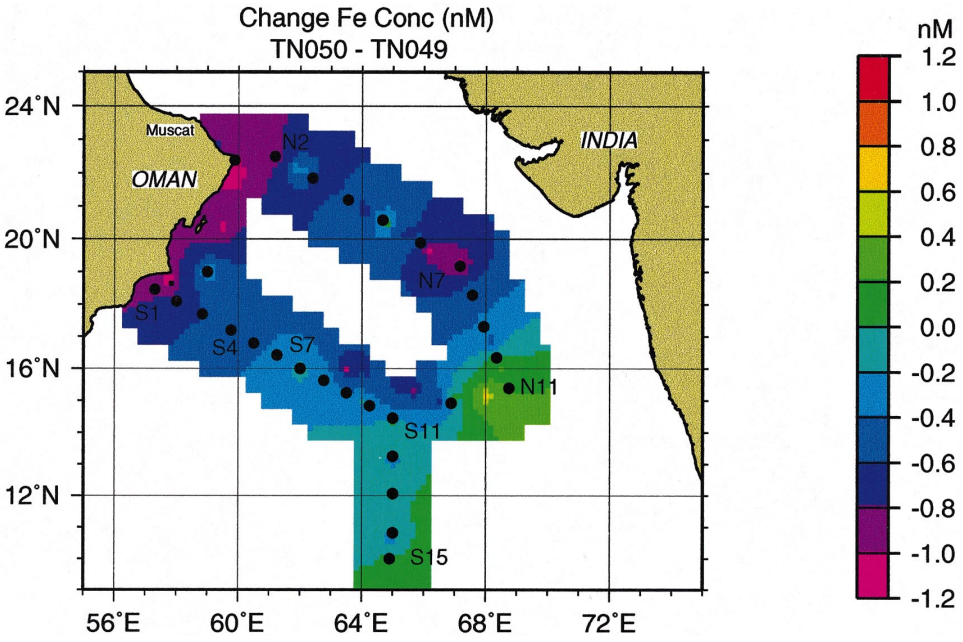

Fig. 5. Contour plot of the differences between the gridded, mixed-layer Fe concentration of TN050 and those of TN049. Standard station locations are shown by (•) and the location of selected stations are noted by text.

1–2 nM towards the east. The overall changes were ~ 0–0.2 nM in southern section and 0.2–0.6 nM in the northern section.

4. Discussion

The observed distributions of dissolved Al and Fe and the changes between the cruises can be interpreted as a dynamic balance between the various addition and removal processes that are occurring during the seasonal cycle. On the input side, the main processes affecting mixed layer concentrations of Al and Fe in the AS are the deposition and partial dissolution of eolian material in the surface waters, and the upwelling of sub-surface water during the SW Monsoon. On the removal side is the incorporation of dissolved material into the particulate phase (primarily biological material associated with the development of phytoplankton blooms during the Southwest Monsoon), and its net removal by vertical transport. Entrainment of water during mixed layer deepening can also affect concentrations. Estimates of the relative role that each of these processes play in controlling the observed distributions are examined in light of existing knowledge of the AS system and the observations of these processes in other parts of the World's ocean.

4.1. Comparison with previous data

Previous Al data from the Arabian Sea (Upadhyay and Sen Gupta, 1994) show strikingly different distributions from those presented here. During January 1988 (NE Monsoon), they found Al Concentrations of 47–52 nM in the region of our stations M1 and N11, and 40–50 nM in the region of N8 and N9, as opposed to our range of 7.7–10 nM between N7 and N11. Additionally, they present deep water ($>$ 2000 m) Al values of $\sim$ 20 nM near N8 and 30–35 nM near N11 compared to our (unpublished) values of 5–10 nM in this region. It is unlikely that these differences are the result of methodology since both sets of data were produced using variants of the Hydes and Liss (1976) method. While sample contamination could result in the higher values, it is also possible that the differences are the result of interannual variations in this dynamic region. Even higher Al values in the surface micro-layer and upper 1 m are reported by Narvekar and Singbal (1993) using a different analytical technique. These authors report Al values of 46–300 nM near N11–N7 during July 1987 and 30–100 nM near N7–N11 during November 1988 for unfiltered samples. Again, interannual monsoon variation may be responsible for these large differences between our data sets; however, it should be noted that some of their values are higher than any reported elsewhere in the surface ocean, including the Mediterranean Sea, which receives considerably greater dust input than the Arabian Sea. Lunel and Statham (pers. comm.), in a transect from 6°S 51°E to 27°S 57°E in August 1986, show surface water Al values ranging from 1.3 to 7.9 nM, and deep water values of 2–4 nM. Despite disagreement between the absolute Al concentrations, we note that the data of both Upadhyay and Sen Gupta (1994) and Narvekar and Singbal (1993) show a significant increase in Al concentrations towards the coast of India. This pattern is consistent with our observed deposition calculations (detailed below), and would provide the anomalously high Al values we observe in the water advected into the extreme southern part of our cruise track during TN049 (see below).

For Fe, there are also few data available for the Arabian Sea. Saager et al. (1992) reported Fe concentrations of 0.30–2.33 nM in the upper 50 m at a station near our N4 during the Fall of 1986. Our values for this station range from 0.8 to 2.3 nM over the same depth range. Takeda et al. (1995) report surface water Fe concentrations of 0.23 nM in the region of our station S11 and 0.36 near N5 for December 1992. Our values for these stations are significantly higher at 0.88 and 1.94 nM. With such a small data base and little sampling over extended periods in this dynamic region, it is difficult to know how much these differences may reflect interannual variations or systematic differences in the analytically determined fractions.

4.2. Systematics of the input and partial dissolution of eolian material

The SW Monsoon is known to generate large dust storms in the desert regions of Africa and the Arabian peninsula and to advect this lofted material into the AS (Husar et al., 1997). In the equatorial Atlantic Ocean, partial dissolution of Saharan dust deposited in surface waters has been recognised as the main phenomenon controlling surface water Al concentrations (Measures and Edmond, 1990). In the case of Al, the

effect of dust input on surface water is large since crustal materials are generally about 8.0% Al by weight and partial dust solubility's for Al are high, ranging from 1.5 to 10% (Prospero et al., 1987; Maring and Duce, 1987). Also the short residence time of Al in surface waters (Orians and Bruland, 1985) results in low background concentrations in surface waters. We can also expect surface Fe concentrations to be enriched by these inputs since crustal materials are typically of the order of 4.3% Fe by weight (Wedepohl, 1995) and partial dust solubilities for Fe in aerosols averages 6.2% (Zhu et al., 1997). However, since Fe appears to be recycled in surface waters, and has limited solubility under oxygenated conditions, ~ 0.2–0.3 nM at pH 8, and up to several nanomolar in the presence of organic complexing agents (Millero, 1998) we expect iron concentrations to respond differently from those of Al.

In our data set, the major changes seen in the surface waters of the AS for both Al and Fe occur during the SW Monsoon (TN049 and TN050) and appear to be related to the processes of eolian deposition and biological removal. The shape of A1 profiles (Fig. 4) showing enhanced Al concentrations in the mixed layer during TN049 further confirms an eolian source of Al to surface waters during this cruise. Upwelling also plays a role in modifying surface water values, although this effect is restricted to the Omani margin where upwelling brings water with Al of ~ 8 nM and Fe ~ 1 nM to the surface during the SW Monsoon.

To determine the feasibility of eolian deposition as the source of the enhanced levels of Al in the surface waters, we can use the excess Al seen in the mixed layer during TN049 compared to TN043 to estimate the amount of dust deposited on the surface waters and then compare these estimates to existing dust deposition data for the region. We will make this estimate using the surface Al values from TN043 as the baseline, since TN045, while closer to the start of the Southwest Monsoon has significantly less coverage.

The average mixed layer Al value for N7–N11 during TN043 is 8.8 ± 1.1 nM, and the average for TN049 is 14.4 ± 1.4 nM, yielding a net increase of 5.6 nM Al. The average depth of the mixed layer in this region during TN049 is 52 m, which implies a total addition to the mixed layer of this region of 291 μmol Al m^{-2} of surface ocean. Assuming either 1.5 or 5% solubility of dust (Measures and Brown, 1996) containing 8.2% Al by weight (Taylor, 1964), we calculate deposition of 2.0–6.8 g dust m^{-2} to the ocean surface between TN043 and TN049 (~ 7 months). Despite the fact that dust sources during this period vary from India to North Africa, the relatively constant Al content of crustal material (8.23 ± 0.53%; Taylor, 1964) introduces negligible error into this calculation. It should be noted that implicit in this calculation is that the water of the mixed layers at stations N7–N11 has not moved during this period, nor has there been any removal of Al from the mixed layer during this period. Clearly neither of these assumptions is true, but we will attempt to estimate the likely errors associated with making them.

In the case of mixed layer changes, a deepening of the mixed layer between TN043 and TN049 could also lead to increases in A1 concentrations as a result of entrainment of deeper waters with higher Al concentrations. However, between TN043 and TN049 most mixed layer depths become shallower. The few exceptions to this are at stations N4–N6 and at S15 and S14. Vertical profiles at these stations during TN043

show no significant increase in Al concentration over the depth range of the deepened mixed layer, and therefore we can rule out any appreciable contribution to the enhanced Al signal during TN049 from this source.

With regard to water motion, Shetye et al. (1994), using Culter and Swallow's (1984) ship drift data, show a weak easterly drift in this region during this period. In contrast, Flagg and Kim (1998) note that ship drift may be unduly biased by wind effects in regions of persistent monodirectional winds (e.g., SW Monsoon); they indicate that surface flows of this region were dominated by mesoscale eddies during this period. The magnitude of the error resulting from making this no surface water motion assumption depends on the true initial value of Al in this water mass before eolian deposition. The lowest values of Al seen in the AS during TN043 and TN045 are ~ 3 nM Al at the western end of the southern section. Thus, if there has been strong advection of the surface layer from the SW bringing this water with the lowest Al values seen during TN043 or TN045 into the region of N7–N11, this could result in a maximum underestimate of the Al input by as much as 5.8 nM, equivalent to an underestimate in dust input of 2.2–7.3 g dust m^{-2} (for 5% or 1.5% solubility, respectively).

With regard to removal of dissolved Al from the water column between TN043 and TN049, initial estimates have been attempted. Using the particulate Th export at 100 m (K. Buesseler, pers. comm., 1997) and assuming 90% of the Al is present in the dissolved load (Broecker and Peng, 1982), an estimate of Al flux from the photic zone can be made between the beginning of TN043 and the beginning of TN049. This calculation suggests that as much as 5.4 to 8 nM Al may be removed along with exported biological material from the surface waters. This would then imply that during this period an extra 1.7–8 g dust m^{-2} (using 5 and 1.5% solubilities, respectively) could have been deposited on the surface ocean. The degree to which this calculation can be validated and refined will be explored in a future publication when initial interpretations of AS data have been completed.

At this stage we will utilise the no-water motion, no-uptake hypothesis to calculate depositions, recognising that they are probably underestimates. Using this approach we can calculate dust deposition to other parts of AS using two different approaches. In the first (Table 2), we use the values of individual stations that were occupied during both TN043 and TN049. In the second, we subtract the gridded Al data used for contouring TN043 from the equivalent for TN049. The advantage of the contouring approach is that we can increase the data base significantly by including underway surface samples and other samples from stations that do not have repeat sampling. The disadvantage is that we are now using data that have been effectively smoothed and interpolated by the contouring operation. We present these data (Fig. 6) as a contour plot of estimated dust deposition using the approach outlined above assuming 1.5% solubility. If 5% solubility were used, the resulting contours would be a factor of 3.3 lower than shown in Fig. 6.

The dust depositions from station-by-station values in Table 2 show somewhat variable inputs along the southern section, with 1.5% solubility-based values ranging from 1.4 to 8.3 g m^{-2}. Much of this variance is the result of mesoscale features present during one or other of the cruises. Gridded distributions (Fig. 6) in general show

Table 2
Implied dust depositions between TN043 and TN049

Station range	Implied dust deposition (g m^{-2})	
	Fractional solubility	
	5%	1.5%
N7–N11	2.2 ± 1.3	7.4 ± 4.3
S15–S13	1.94 ± 0.24	6.5 ± 0.8
S11–S10	1.54 ± 0.4	5.12 ± 1.3
S7	0.43	1.43
S5–S4	0.79 ± 0.04	2.63 ± 0.13
S3	2.5	8.3
S2–S1	0.48 ± 0.06	1.6 ± 0.2

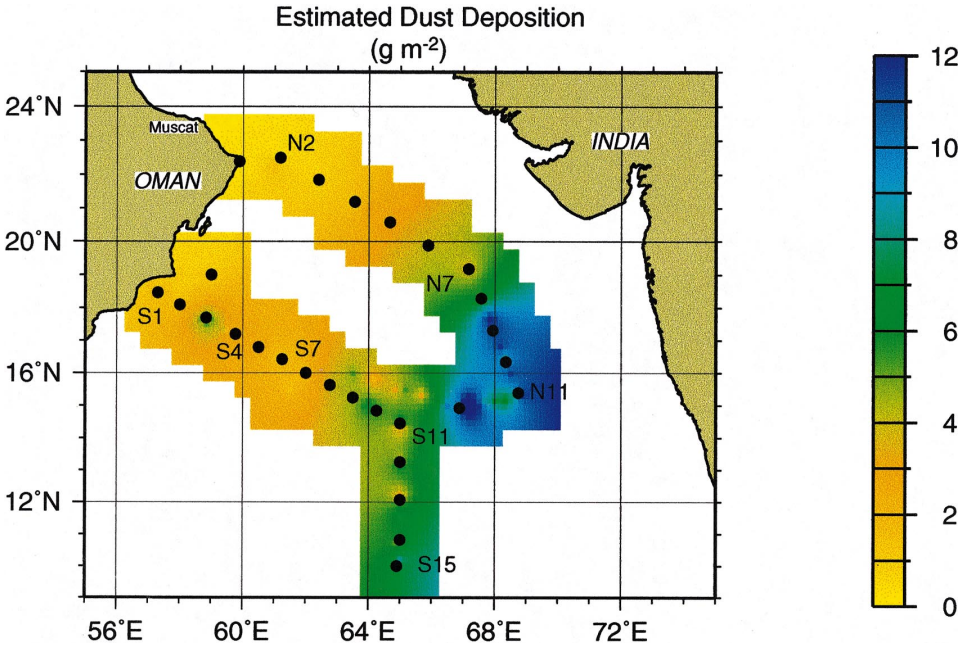

Fig. 6. Contour of the estimated dust deposition to the Arabian Sea using gridded data from TN049 and TN043 (see text for details). Standard station locations are shown by (•) and the location of selected stations are noted by text.

similar values but, as expected, are somewhat smoother. Regional differences do occur between the estimates though, such as in the eastern part of the AS where the inclusion in the gridded data of a large number of underway surface samples with high Al concentrations increase estimates of dust deposition in this region by 2–3 g m^{-2}.

Overall, the results indicate that implied dust depositions range from 2.2–7.4 g m^{-2} in the NE to 0.43–1.6 g m^{-2} in the southwest coastal region.

The apparent greater input of dust into surface waters of the NE part of the AS compared with the S and SW during the SW Monsoon could be real or the result of one of several artifacts. First, in the S and SW regions there is a much greater problem of underestimation of the original Al values in the surface waters because of the mesoscale variability in this region as well as the significantly higher horizontal advection rates. For example, S7 in Table 2 shows much lower deposition than the nearby stations S5 and S4 due to the presence of an eddy with low Al at S6 and S7 during TN049. The process of upwelling along the Omani coast (as mentioned above) brings water with a higher (~ 8 nM) Al content to the surface than the 3 nM observed at the surface in this region during TN043. Since this enhanced Al is not a result of eolian deposition to these surface waters, the dust inputs calculated from Al differences are not reliable in this region. In fact, since surface water Al values during TN049 match those of the source waters for the upwelling region, we would calculate zero dust deposition along the coast. The unexpected and extremely high deposition values calculated at S15 are believed to be the result of a similar effect, the advection of high Al water into this region from the west during TN049. Morrison et al. (1998) show evidence for this advection and if the Al gradients in the data of Upadhyay and Sen Gupta (1994) and Narvekar and Singbal (1993) are correct, then we would expect water from the west to have a much higher original Al content, leading to an overestimate of dust deposition.

Despite these caveats, the asymmetric enrichment of Al in the surface waters of the region may be the result of real dust input. Inspection of global analyses of monthly precipitation derived from satellite and surface measurements for this region (Huffman et al., 1997) indicate that during the SW Monsoon there is a very strong East–West gradient in precipitation across the AS. Values of < 15 mm $month^{-1}$ in the western AS increase to > 450 mm $month^{-1}$ in the eastern part of the AS. This gradient is driven by orographic precipitation over the Western Ghats along the west coast of India. Since wet deposition, when operative, is the most efficient means of removing dust from the atmosphere, a gradient in rainfall also could lead to a gradient in dust deposition to the surface ocean. However, it should be noted that the precipitation gradient reported over the AS is derived from a variety of satellite sensors and there are few direct measurements to confirm this gradient. When available, precipitation data from the AS cruises may be useful in determining whether such a gradient exists.

Tindale and Pease (1999) showed that the air above the marine boundary layer of the AS during the SW Monsoon comes from areas to the Northeast and East of the AS. These air mass back trajectory calculations combined with the high aerosol optical depths determined from satellite observations during the SW Monsoon (Husar et al., 1997), and the rainfall gradient noted above, are consistent with the observed pattern of enrichment of Al in the surface waters of the AS. Such a rainfall and dust gradient also would be consistent with pattern of surface water distributions observed by Upadhyay and Sen Gupta (1994) and Narvekar and Singbal (1993).

Despite the many uncertainties that result from the assumptions in the calculation outlined above, we can compare our estimated dust inputs with historic estimates of dust deposition to this region, since direct dust deposition estimates are not yet available for the JGOFS study period. Chester et al. (1991), using measured suspended dust loads and calculated deposition velocities and an assumed distribution between wet and dry deposition, calculated an annual deposition ~ 10 g dust m^{-2} yr^{-1} to the AS. This value is close to the long-term accumulation rates of lithogenic materials in this region reported by Prell et al. (1980) equivalent to 13 g m^{-2} yr^{-1} and by Goldberg and Griffin (1970) of 10.6 g m^{-2} yr^{-1}. Our calculated dust depositions appear to be somewhat lower but reasonably close to historic estimates. Initial data from the lithogenic component in sediment traps deployed during the Arabian Sea expedition along the southern section (J. Dymond, pers. comm., 1997) indicate mineral dust accumulations of 1.5 to 5.4 g m^{-2} between January and August 1995, with lowest values around S15 and higher values to the west around S3. While our spatial trends are somewhat different, perhaps as a result of the artifacts of upwelling and advection mentioned above, the magnitudes of dust deposition we calculate are similar, and within the normal factor of two uncertainty common in this measurement.

4.3. Estimating the magnitude of eolian deposition of Fe

In principal, the eolian deposition of Al also can be used to estimate the eolian deposition of Fe to the surface water, thus allowing some estimate of the flux of Fe to the surface of the AS by this process. However, as we show below, solubility of Fe may be controlling the total amount of Fe that enters the dissolved phase and, therefore, it is difficult to make a quantitative estimate of Fe deposition at this stage.

The Al/Fe molar ratio in mineral dust collected during this study varied between 1.5 and 4.2 (mean 2.8), with the lowest values being observed during the Southwest Monsoon (Tindale and Pease, 1999). Congruent dissolution of this material would yield a similar Al/Fe molar ratio in surface waters of the AS of 1.5–4.2. For higher partial solubilities of iron (values up to 13% are reported by Zhu et al., 1997), the Al/Fe ratio in surface waters will be lower. For example, while using 5% Al solubility and 6.2% Fe solubility, the mean value reported by Zhu et al. (1997), would yield an Al/Fe ratio of 1.2 in surface waters.

The observed dissolved Al/Fe concentration ratios in the surface waters of the AS vary from ~ 3 in the Omani coastal region during the NE Monsoon to ~ 18–24 in the NE region during the SW Monsoon. High Al/Fe values in regions of dust deposition are not limited to the AS. In a region of the equatorial Atlantic Ocean believed to receive large dust inputs (Duce et al., 1991; Prospero, 1996), observed values for the Al/Fe in the surface ocean range up to 90 (Vink and Measures, 1999). In the Pacific Ocean north of Hawaii, Al/Fe values are up to 16 (Tersol et al., 1996). In each of these cases the Al/Fe values are a factor of 3–20 higher than those predicted using estimated solubilities. Differential scavenging and removal of the two elements from surface waters are unlikely to be the cause of the high Al/Fe values observed. Irreversible scavenging and removal of Al (Measures and Edmond, 1990; Moran and

Moore, 1988), when coupled with a high degree of recycling of Fe in surface water biological reservoirs (Hutchins et al., 1993), would be expected to reduce the Al/Fe ratio with time, not increase it.

It also seems unlikely that these high values are a result of underestimation of the partial solubility of Al since reported values rarely exceed 9% (Prospero et al., 1987; Maring and Duce, 1987). To achieve an Al/Fe of 30 with 6.2% Fe solubility (Zhu et al., 1997), an unsustainable 64% fractional solubility for Al would be required.

Clearly, the problem must lie in the observed fractional solubility of Fe in dust. If the high Al/Fe values are the result of overestimation of the Fe partial solubilities, then, to produce a surface water Al/Fe value of 30 assuming partial Al solubility of 5%, the Fe partial solubility would be only 0.5%, a factor of 6 to 26 times lower than the 3–13% reported values (Zhu et al., 1997). It seems probable that Fe dissolving in large amounts from particulate material (dust), is being rapidly removed from the 0.2 μm filtered dissolved phase that we measure either by incorporation into biological phases, by re-scavenging onto dust, or by formation of phases retained by the filter.

While removal of Fe into biological materials is clearly occurring, estimates of the standing crop during TN049 and assuming a C : Fe compositional ratio (Sunda and Huntsman, 1995) indicate only $\sim$ 10% of the iron is associated with this phase. Also, since Fe is recycled rapidly only a permanent increase in the steady state biomass or export of Fe from the euphotic zone can raise the Al/Fe value. In this latter case, the removal ratio of Fe to Al also would have to be higher than the input ratio. It seems more likely that dissolved Fe concentrations are being controlled on a more rapid time scale by scavenging of dissolved Fe or the formation of insoluble phases, and that the effective solubility of Fe in seawater is much lower than the 6.2% value would imply.

This explanation is consistent with the results of Zhu et al. (1997). These authors found that the fraction of soluble Fe in Saharan aerosols was generally higher during periods of lower dust load. The observation of solubility control in laboratory experiments suggests that this also may be controlling Fe input in the field and may be the cause of the unexpectedly high Al/Fe values in the AS and elsewhere. With solubility control on the Fe input, the Al/Fe ratio will scale with the amount of dust going into the ocean since there is an upper limit on the amount of Fe that can enter the dissolved phase. The Al/Fe ratio is highest in the equatorial Atlantic Ocean (up to 90; Vink and Measures, submitted), where the dust input is highest (5–10 g m^{-2}; Prospero, 1996). It is lower in the AS (up to 26; this work), where dust input appears to be in the range 2–7 g m^{-2} (Chester et al., 1991), and is lower still in the Pacific Ocean (up to 16; Tersol et al., 1996), where dust inputs are lowest (0.4 g m^{-2}; Uematsu et al., 1994). Here, we are implicity assuming that there is no solubility control on the partial dissolution of Al, as a matter of practicality rather than known veracity. However, Al concentrations of up to 170 nM, much higher than those observed here, have been found in the Mediterranean Sea (Hydes et al., 1988).

With Fe input under solubility control, it is more difficult to calculate the net input of Fe to the surface water as the result of dust deposition. However, despite this difficulty it is clear from Fig. 3 that Fe concentrations increased in surface waters of

the AS between TN043 (January) and TN049 (July). The increases range from $+0.2$ nM in the northern (N3–N6) and southern (S11–S1) sections to $+0.5$ nM between N7 and N12. Large apparent increases in Fe between S14 and S11 ($+0.3$ nM) are probably the result of the advection of high Fe water into the region (described above for Al). Increases of up to 0.9 nM Fe are seen in the Omani coastal region, particularly in the north around the mouth of the Gulf of Oman. These concentration increases are equivalent to the addition of between 8 and 9 μmol Fe m^{-2} to the mixed layer in the regions between N3–N6 and between S11–S1, 24 μmol Fe m^{-2} in the northeast region between stations N7–N12, and of ~ 14 μmol Fe m^{-2} to the shallower mixed layers of the coastal region. With the exception of this latter region, the pattern of input (i.e., greatest in the eastern part of the study area) is similar to that of the estimated eolian dust deposition calculated from Al (Fig. 6).

In addition to the eolian deposition, upwelling of sub-surface waters along the Omani coast during the SW Monsoon also provides Fe to the surface waters. Although Fe values are high in the sub-surface, sub-oxic waters along the Omani margin (> 1.8 nM below 60 m at S1 during TN050), Morrison et al. (1998) using temperature and Si/NO_3 values have shown that the upwelled water originates from depths of 120–150 m in the western part of the southern section where Fe levels are significantly lower (~ 1 nM). At this stage, without independent estimates of the amount of water upwelled during the SW Monsoon, it is not possible to calculate the potential flux from this source or its importance relative to the eolian flux. We will return to the subject of the relative roles that upwelling and eolian deposition play in providing iron to support export production after discussing the Fe removal process.

4.4. The role of biological uptake in removing dissolved iron

The requirement for Fe in marine phytoplankton has been well documented, as well as its role in limiting production in certain remote parts of the ocean (Martin and Fitzwater, 1988; Bruland et al., 1991; Sunda and Huntsman, 1995; Wells et al., 1995). Although the AS is not an Fe-limited ocean, the removal of Fe from the dissolved pool into the particulate pool during the growth of the monsoon-induced blooms, and its subsequent removal from the euphotic zone as a result of the export of organic matter, is expected to play a significant role in the Fe budget of the upper waters of the AS.

We can examine the disappearance of Fe from the dissolved phase between cruises TN049 and TN050, when export production estimated from Th deficits was shown to increase dramatically (Buesseler et al., 1998). The average Fe concentration during TN049, using all data between N4–N9, is 1.4 ± 0.5 nM, and for TN050 it is 0.9 ± 0.2 nM. The net removal then is ~ 0.5 nM Fe. The average mixed layer depth across these stations is 55 ± 8 m, implying a net removal of ~ 30 μmol Fe m^{-2}. If this Fe were removed by incorporation into phytoplankton with C : Fe molar ratios of 10^5 (Sunda and Huntsman, 1995), then this would imply the production (and removal from the dissolved phase) of 3 mol C m^{-2} in the mixed layer during this one month period. It is interesting to note that TOC values in the upper 150 m indicate an integrated removal of 2 mol C m^{-2} over the AS between TN049 and TN050 (Hansell and Peltzer, 1998).

A similar removal of Fe from the dissolved phase is seen along the Omani margin (using all stations between S5 and Arabesque (A)). Values in the upper waters drop from an average 1.5 ± 0.5 nM Fe during TN049 to 0.74 ± 0.05 nM Fe during TN050. Since the average mixed layer (17 ± 12 m) in this region is much shallower, the absolute magnitude of Fe removal is smaller (~ 13 μmol m^{-2}) than in the northern region, and would be the equivalent of the formation of 0.13–1.3 mol C m^{-2} during this period. Detailed coupling of export production with changes in dissolved Fe levels will be addressed in a later publication.

4.5. The importance of eolian deposition to upwelling systems

Even though we are unable to quantify the fluxes of Fe to the surface waters through upwelling at this stage, we can compare the upwelled supply to that needed to support export production through its ratio to NO_3. Systems are considered Fe-limited if the C : Fe exceeds $10^5 : 1$ and Fe replete if the C : Fe is less than $10^5 : 1$ (Sunda and Huntsman, 1995). Using C : N value of 6.67 we can calculate that this is equivalent to N : Fe of $> 15{,}000 : 1$ for Fe limited and $< 15{,}000 : 1$ for Fe replete systems. The water upwelling at S1 in TN050 has an NO_3/Fe value between 20,000 and 30,000 : 1, well above the Fe limiting value. Thus, despite the fact that Fe-rich water is being upwelled into the surface layer, an additional Fe input, presumably supplied by the eolian deposition, is required to bring the N : Fe ratio below that at which Fe limitation of growth begins to appear. Had the upwelling drawn water from the sub-oxic zone of the water column, where Fe concentrations are > 1.8 nM, and the NO_3/Fe ratio is $< 14{,}000 : 1$, surface waters would be below the ratio where Fe limitation begins.

The separation of N and P from Fe during remineralisation of organic carbon in the oxic ocean is probably primarily responsible for development of low Fe conditions in the high-nutrient, low-chlorophyll *a* regions. In contrast, in regions where the primary site of organic matter diagenesis is poorly ventilated and Fe solubility is much higher, this separation is less pronounced and the stoichiometric relationship between Fe and the major nutrients can be maintained. However, unless suboxic water with its high levels of Fe is upwelled, an external input of Fe is always required to balance upwelled sources of nutrients. While this Fe may be supplied by sedimentary sources in shallow coastal regions, in the open ocean only eolian deposition can supply the required Fe. We can expect that wind-driven upwelling in oceanic regions remote from eolian dust input will always be Fe-limited.

5. Summary

Concentrations of Al and Fe dissolved in surface waters of the Arabian Sea increased dramatically in response to the deposition and partial dissolution of dust during the Southwest Monsoon. Scavenging of dissolved Al and rapid export of particles from the mixed layer during the later part of the Southwest Monsoon dramatically reduced the concentration of Al dissolved in the surface waters. Iron

concentrations showed less variation than Al between cruises due to solubility control of dissolved Fe concentrations and biological recycling of this element within the mixed layer.

Calculated dust deposition rates using dissolved Al were generally similar to the historical and contemporary estimates of dust deposition determined for this area using aerosol concentrations, sediment cores and sediment traps (Chester et al., 1991; Prell et al., 1980; Goldberg and Griffin, 1970; J. Dymond, pers. comm., 1997). Dust deposition was greatest in the northeast section of the cruise track during the Southwest Monsoon. The spatial and temporal distribution of deposition is also consistent with calculated air mass back trajectories and rainfall estimates for this region. Estimates of dissolved Fe input from the dust to the surface ocean are problematic due to the solubility control of dissolved Fe concentrations.

Eolian deposition appears to be very important in supplying Fe to the remote surface ocean particularly in areas where upwelling nutrient supply is not drawn from a sub-oxic layer.

Acknowledgements

We would like to thank Rebecca Reitmeyer and Shevaun Fennel for their contribution to the sea-going component of this work. We are also grateful to Sharon Smith for the immense effort she put into organising the Arabian Sea project. Thoughtful and detailed reviews by Bill Sunda and two anonymous reviewers have improved the manuscript and we gratefully acknowledge their efforts. We would like to thank the officers and crew of the R.V. *T.G. Thompson* for their professional skills which helped ensure the success of the project as well as our underway sampling program. Finally we would like to thank collectively all of the other participating scientists in the Arabian Sea project for their many acts of collaboration, generosity and support throughout a very long field season on a very crowded ship. Support for this work was provided by the National Science Foundation grant # OCE 93-10943, development of the underway FIA system was supported by the Office of Naval Research grant #N00014-92-J-1485. This is contribution # 4801 of the School of Ocean Earth Science and Technology, University of Hawaii and JGOFS contribution # 424.

References

Banse, K., 1994. On the coupling of hydrography, phytoplankton, zooplankton, and settling organic particles offshore in the Arabian Sea. In: Lal, D. (Ed.), Biogeochemistry of the Arabian Sea. Indian Academy of Sciences, pp. 27–63.

Broecker, W.S., Peng, T.H., 1982. Tracers in the Sea. Eldigio Press, New York, 689 pp.

Bruland, K.W., Donat, J.R., Hutchins, D.A., 1991. Interactive influence of bioactive trace metals on biological production in oceanic waters. Limnology and Oceanography 36, 1555–1577.

Buesseler, K., Ball, L., Andrews, J., Benitez-Nelson, C., Belastock, R., Chai, F., Chao, Y., 1988. Upper ocean export of particulate organic carbon in the Arabian Sea derived from thorium-234. Deep-Sea Research II 45, 2461–2488.

Chester, R., Berry, A.S., Murphy, K.J.T., 1991. The distribution of particulate atmospheric trace metals and mineral aerosols over the Indian Ocean. Marine Chemistry 34, 261–290.

Coale, K.H., et al., 1996. A massive phytoplankton bloom induced by an ecosystem-scale iron fertilization experiment in the equatorial Pacific Ocean. Nature 383, 495–501.

Duce, R.A. et al., 1991. The atmospheric input of trace species to the World Ocean. Global Biogeochemical Cycles 5, 193–259.

Duce, R.A., Tindale, N.W., 1991. Atmospheric transport of iron and its deposition in the ocean. Limnology and Oceanography 36, 1715–1726.

Flagg, C.N., Kim, H.S., 1998. Upper ocean currents in the northern Arabian Sea from shipbpoard ADCP measurements collected during the 1994–1996 JGOFS and ONR programs. Deep-Sea Research II 45, 1917–1960.

Golberg, E.D., Griffin, J.J., 1970. The sediments of the northern Indian Ocean. Deep-Sea Research 17, 513–537.

Hansell, D.A., Peltzer, E.T., 1998. Spatial and temporal variations of total organic carbon in the Arabian Sea. Deep-Sea Research II 45, 2171–2194.

Hunter, C.N., Gordon, R.M., Fitzwater, S.E., Coale, K.H., 1996. A rosette system for the collection of trace metal clean seawater. Limnology and Oceanography 41, 1367–1372.

Husar, R.B., Prospero, J.M., Stow, L.L., 1997. Characterization of tropospheric aerosols over the oceans with the NOAA advanced very high resolution radiometer optical thickness operational product. Journal of Geophysical Research 102(D14), 16889–16909.

Hutchins, D.A., DiTullio, G.R., Bruland, K.W., 1993. Iron and regenerated production: evidence for biological iron recycling in two marine environments. Limnology and Oceanography 38, 1242–1255.

Hydes, D.J., Liss, P.S., 1976. A fluorometric method for the determination of low concentrations of dissoved aluminium in natural waters. Analyst 101, 922–931.

Hydes, D.J., de Lange, G.J., de Baar, H.J.W., 1988. Dissolved aluminium in the Mediterranean. Geochimica et Cosmoschimica Acta 52, 2107–2114.

Kremling, K., 1985. The distribution of cadmium, copper, nickel, manganese, and aluminium in surface waters of the open Atlantic and European shelf area. Deep-Sea Research 32, 531–555.

Maring, H.B., Duce, R.A., 1987. The impact of atmospheric aerosols on trace metal chemistry in open ocean surface seawater, 1, Aluminium. Earth and Planetary Science Letters 84, 381–392.

Martin, J.H., Fitzwater, S.E., 1988. Iron deficiency limits phytoplankton growth in the north-east subarctic Pacific. Nature 331, 341–343.

Martin, J.M., Gordon, R.M., Fitzwater, S.E., 1990. Iron in Antarctic waters. Nature 345, 156–158.

Martin, J.H., et al., 1994. Testing the iron hypothesis in ecosystems of the equatorial Pacific Ocean. Nature 371, 123–129.

Measures, C.I., Brown, E.T., 1996. Estimating dust input to the Atlantic Ocean using surface water Al concentrations. In: Guerzoni, Chester (Eds.), The impact of African Dust Across the Mediterranean. Kluwer, Dordrecht, pp. 389–402.

Measures, C.I., Edmond, J.M., 1990. Aluminium in the South Atlantic: steady state distribution of a short residence time element. Journal of Geophysical Research 95, 5331–5340.

Measures, C.I., Edmond, J.M., Jickells, T.D., 1986. Aluminium in the North West Atlantic. Geochimica et Cosmochimica Acta 50, 1423–1429.

Measures, C.I., Yuan, J., Resing, J.A., 1995. Determination of iron in seawater by flow injection analysis using in-line preconcentration and spectrophotometric detection. Marine Chemistry 50, 3–12.

Millero, F.J., 1998. Solubility of Fe III in seawater. Earth and Planetary Science Letters 154, 323–329.

Moran, S.B., Moore, R.M., 1988. Temporal variations in dissolved and particulate aluminium during a spring bloom. Estuarine Coastal and Shelf Science 27, 205–215.

Morrisson, J.M., Codispotti, L.A., Gaurin, S., Jones, B., Manghnani, V., Zheng, Z., 1998. The hydrographic mileu of the US JGOFS Arabian Sea Process Experiment. Deep-Sea Research II 45, 2053–2102.

Narvekar, P.V., Singbal, S.Y.S., 1993. Dissolved aluminium in the surface microlayer of the eastern Arabian Sea. Marine Chemistry 42, 85–94.

Prell, W.L., Hutson, W.H., Williams, D.F., Be, A.W.H., Geitzenauer, K., Molfino, B., 1980. Surface circulation of the Indian Ocean during the last glacial maximum, approximately 10,000 yr. B.P. Quaternary Research 14, 309–336.

Prospero, J.M., 1996. Saharan dust transport over the North Atlantic Ocean and Mediterranean: an overview. In: Guerzoni, Chester (Eds.), The Impact of African Dust Across the Mediterranean. Kluwer, Dordrecht, pp. 133–152.

Prospero, J.M., Nees, R.T., Uematsu, M., 1987. Deposition rate of particulate and dissolved aluminium derived from Saharan dust in precipitation at Miami, Florida. Journal of Geophysical Research 92, 14723–14731.

Resing, J., Measures, C.I., 1994. Fluorometric determination of Al in seawater by FIA with in-line preconcentration. Analytical Chemistry 66, 4105–4111.

Shetye, S.R., Gouveia A.D., Shenoi, S.S.C., 1994. Circulation and water masses of the Arabian Sea. In: Lal, D. (Ed.), Biogeochemistry of the Arabian Sea. Indian Academy of Science, pp. 9–25.

Smith, W.H.F., Wessel, P., 1990. Gridding with continuous curvature splines in tension. Geophysics 55, 293–305.

Statham, P., Burton, J.D., 1986. Dissolved manganese in the North Atlantic Ocean. Earth and Planetary Science Letters 79, 55–65.

Sunda, W.G., Huntsman, S.A., 1995. Iron uptake and growth limitation in oceanic and coastal phytoplankton. Marine Chemistry 50, 189–206.

Sunda, W.G., Huntsman, S.A., 1997. Interrelated influence of iron, light and cell size on marine phytoplankton growth. Nature 390, 389–392.

Takeda, S., Kamatani, A., Kawanobe, K., 1995. Effects of nitrogen and iron enrichments on phytoplankton communities in the northwestern Indian Ocean. Marine Chemistry 50, 229–241.

Taylor, S.R., 1964. Abundance of chemical elements in the continental crust: a new table. Geochimica et Cosmochimica Acta 28, 1273–1285.

Tersol, V., Vink, S., Yuan, J., Measures, C.I., 1996. Variations in Iron, Aluminium and Beryllium concentrations in surface waters at Station Aloha. EOS Transactions of the American Geophysical Union 76, OS65.

Tindale, N., Pease, P.O., 1999. Aerosols over the Arabian Sea: Atmospheric transport pathways and concentrations of dust and sea salt. Deep-Sea Research II 46, 1577–1595.

Uematsu, M., Duce, R.A., Prospero, J.M., Chen, L., Merrill, J.T., McDonald, R.L., 1994. Transport of mineral aerosol from Asia over the North Pacific Ocean. Journal of Geophysical Research 88, 5343–5352.

Upadhyay, S., Sen Gupta, R., 1994. Aluminium in the northwestern Indian Ocean (Arabian Sea). Marine Chemistry 47, 203–214.

Vink, S., Boyle, E.A., Measures, C.I., Yuan, J.C., 1999. Automated high resolution determination of the trace elements iron and aluminium in the surface ocean using a towed fish coupled to flow injection analysis, in review, Deep-Sea Research.

Vink, S., Measures, C.I., 1999. The role of dust deposition in determining surface water distributions of Fe and Al in the South west Atlantic. Submitted Deep-Sea Research.

Wedepohl, K.H., 1995. The composition of the continental crust. Geochimica et Cosmochimica Acta 59, 1217–1232.

Wells, M.L., Price, N.M., Bruland, K.W., 1995. Iron chemistry in seawater and its relationship to phytoplankton: a workshop report. Marine Chemistry 48, 157–182.

Wessel, P., Smith, W.H.F., 1995. New version of the Generic Mapping Tools released. EOS Transactions of the American Geophysical Union 76, 329.

Zhu, X.R., Prospero, J.M., Millero, F.J., 1997. Diel variability of soluble Fe(II) and soluble total Fe in the North African dust in the trade winds at Barbados. Journal of Geophysical Research 102(D17), 21297–21305.